www.sciencemag.org/content/356/6334/197/suppl/DC1

Supplementary Materials for

Nanoscale-length control of the flagellar driveshaft requires hitting the tethered outer membrane

Eli J. Cohen, Josie L. Ferreira, Mark S. Ladinsky, Morgan Beeby, Kelly T. Hughes*

*Corresponding author. Email: hughes@biology.utah.edu

Published 14 April 2017, *Science* **356**, 197 (2017)
DOI: 10.1126/science.aam6512

This PDF file includes

Materials and Methods

Bacterial Strains, Plasmids and Media

Detailed information about bacterial strains and plasmids used in this study are listed in Table 1. Cells were cultured in Lysis Broth (LB). Media was supplemented with the following antibiotics when needed: chloramphenicol (12.5 μg/mL), kanamycin (50 μg/mL), tetracycline (15 μg/mL), ampicillin (100 μg/mL). Genes expressed from the chromosomal arabinose-inducible *araBAD* promoter (P_{araBAD}) were induced by the addition of L-arabinose (final concentration: 0.2%). All transductional crosses were performed using the generalized transducing phage of Salmonella Typhimurium P22 HT105/1 int-201. λ-Red recombineering (*29*) was performed using tetracycline for selection and anhydrotetracycline/fusaric acid media for subsequent counterselection.

Swimming and Swarming Motility Assays

Swimming motility was assayed by stabbing single colonies into swimming motility plates (0.2% agar with 10 g/L tryptone and 5 g/L NaCl added) and incubated face-up at 37° C for 8-12 hours. For swarming motility assays, 1 µL of overnight cultures were spotted on swarming motility agar (0.5% agar with 10 g/L tryptone, 5 g/L yeast extract, 10 g/L NaCl and 0.5% glucose added) followed by incubating face-up at 37° C for 16-18 hours. Swim diameters were measured using ImageJ 1.50i software (National Institutes of Health (NIH)). Graphs were made with Graphpad Prism 5 software suite (Graphpad software, Inc.)

Isolation, Transmission Electron Microscopy and Measurement of Flagellar Structures

Hook basal body (HBB) isolation was carried out by methods described previously (*30*), with minor modifications. Structures were not collected by CsCl or sucrose gradient centrifugation but were pelleted at 60,000 x g for 1 h using a Beckman 50.2Ti and/or S80-AT3 rotor at 12 °C.

Purified structures were applied to glow discharged carbon-coated formvar copper grids (Cu-FCF-300H grids, Electron Microscopy Sciences) and stained with 2% aqueous phosphotungstic acid (pH ~7.0). Images were captured using a JEOL JEM-1400 electron microscope at an acceleration voltage of 120 kV coupled to a Gatan CCD camera.

Rod lengths were measured using NIH ImageJ 1.50i software. Statistical analysis and graphs were made using the Graphpad Prism 5 software suite (Graphpad software, Inc., Figs. 2, 4D, 4E, S4, S5)

SDS-PAGE Sample Preparation and Immunoblotting

For detection of FliC-3xHA in culture supernatants, overnight cultures were diluted 1:100 in fresh LB and grown at 37° C with aeration to $O.D._{600}$ ~1.0. Cells were harvested by centrifugation and gently resuspended in cold 0.1 M glycine, pH 2.5 and incubated on ice for 20-30 minutes to depolymerize flagellar filaments. Following depolymerization, cells were pelleted by centrifugation and the supernatant carefully decanted. 0.5 µg lysozyme was added to the supernatant to act as a carrier for TCA precipitation. The precipitant was washed twice with cold acetone and boiled in 2x SDS Laemlli buffer. Samples were run on hand-cast, 12% tris-glycine

polyacrylamide gels with 0.1% SDS added. Following SDS-PAGE, proteins were transferred to nitrocellulose by semi-dry transfer and probed with anti-HA and anti-DnaK (a cell lysis control) antisera in TBST with 5% milk added. Following incubation with 1° antibody, membranes were incubated with IRdye fluorescently labeled 2° antibody and developed on a LI-COR Biosciences Odyssey infrared imaging system.

For purification and detection of Lpp linked to cell wall sacculi, cultures were grown overnight in 10 mL of LB at 37° C with aeration. Cells were pelleted, resuspended in 3 mL saline and dripped into 6 mL of 6% SDS heated to 85-90° C with stirring. Lysates were stirred at 85-90° C for 2-3 hours followed by centrifugation at 100,000xg for 1 hour. Pellets were washed 3x with 20 mL H2O to remove all SDS and resuspended in 1 mL PBS. Lysozyme was added to the purified sacculi (final concentration: 2 mg/mL) and incubated at 37° C overnight. Lysozyme digests were concentrated by TCA precipitation and resuspended in 100 µL 2xSDS Laemlli buffer. Typically, 5-10 µL of sample were loaded to 13% tris-tricine polyacrylamide gels. Lpp was detected using anti-Lpp antisera following the protocol described above.

EM Preparation for Resin-embedded Electron Tomography

Salmonella cultures were prepared for EM by high-pressure freezing and freeze-substitution. Cells were briefly centrifuged and the pellets resuspended in culture medium containing 10% Ficoll (70kD; Sigma), which serves as an extracellular cryoprotectant. The cells were centrifuged again and the supernated removed. Pellets of Salmonella cells were transferred to brass freezing planchettes (Ted Pella, Inc.) and rapidly frozen in a HPM-010 high-pressure freezer (Leica Microsystems, Vienna Austria), then stored under liquid nitrogen. The frozen planchettes were subsequently placed in cryotubes (Nunc) containing 2 ml of 2% glutaraldehyde in acetone and transferred to a AFS2 freeze-substitution machine (Leica Microsystems). Samples were freeze-substituted at -90°C for 60 hours, then warmed to -20° C over 8 hours. The samples were then rinsed 3x with cold acetone and processing continued at -20°C for an additional 24 hours with 2.5% OsO_4, 0.05% uranyl acetate in acetone. The samples were then warmed to room temperature, rinsed 4x with acetone and infiltrated with Epon-Araldite resin (Electron Microscopy Sciences, Port Washington PA). Pellets of cells were embedded in plastic sectioning capsules and the resin polymerized at 60°C for 48 hours.

Thick (400 nm) sections were cut with a UC6 ultramicrotome (Leica Microsystems) using a diamond knife (Diatome Ltd., Switzerland). And placed on Formvar-coated copper-rhodium 1mm slot grids (Electron Microscopy Sciences). Sections were stained with 3% uranyl acetate and lead citrate and colloidal gold particles (10 nm) were placed on both surfaces of the grids to serve as fiducial markers for image alignment. Grids were stabilized with evaporated carbon prior to imaging.

Electron Tomography and Peptidoglycan to Outer Membrane Measurement

Grids were placed in a Dual-Axis Tomography holder (Model 2040, Fischione Instruments, Inc., Export, PA) and imaged with a Tecnai TF30ST-FEG microscope (FEI Company, Holland) at 300 KeV. Dual-axis tilt series (+/- 64° at 1° intervals) were acquired automatically using the SerialEM software package 21). Tomographic data were aligned, analyzed and segmented using IMOD (*31-32*, Fig. 4B) on MacPro computers (Apple, Inc).

For measurement of cell wall peptidoglycan (CW) to outer membrane (OM) distances, 3 tomogram sections each of >3 cells per LppA length variant were saved as .tif files and analyzed

in ImageJ (NIH). Distances between the CW and OM were measured every 5-10 nm, for a total of ~200 measurements per length variant, and plotted using Graphpad Prism software (Graphpad software, Inc., Fig. 4A)

Preparation of Electron Cryo-microscopy Samples, Data Collection and Analysis

Strains were grown aerobically in LB at 37° C until an $O.D._{600}$ of 0.6 was reached. Cells were spun for 5 minutes at 6000xg and resuspended to an $O.D._{600}$ of ~18.
UltraAuFoil R2/2 grids (200 mesh) (Quantifoil Micro Tools GmbH) were glow-discharged for 60s at 10mA. Cells were mixed with a solution of 10nm colloidal gold (Sigma) immediately before freezing. A 2.5µl droplet of sample was applied to the grid and plunge frozen using a Vitrobot MkIV (FEI Company) with a wait time of 60s, a blot time of 5s, a blot force of 3 and a drain time of 1s at a constant humidity of 100%. Grids were stored under liquid nitrogen until required for data collection.
Projection images were collected on a 200keV FEI Tecnai TF20 FEG transmission electron microscope (FEI Company) equipped with a Falcon II direct electron detector (FEI Company) using a Gatan 626 cryogenic-holder (Gatan). Leginon automated data-collection software (*33*) was used to acquire images with pixel size of 0.828nm (nominal magnification 25000x) with a defocus of -5µm.
3dmod from the IMOD package (*34*) and custom scripting were used to manually segment inner and outer membranes of projection images of ~25 cells per mutant, measuring the periplasmic width at 0.5nm intervals, resulting in tens of thousands of data points per mutant to produce width histograms (Fig. 4C).

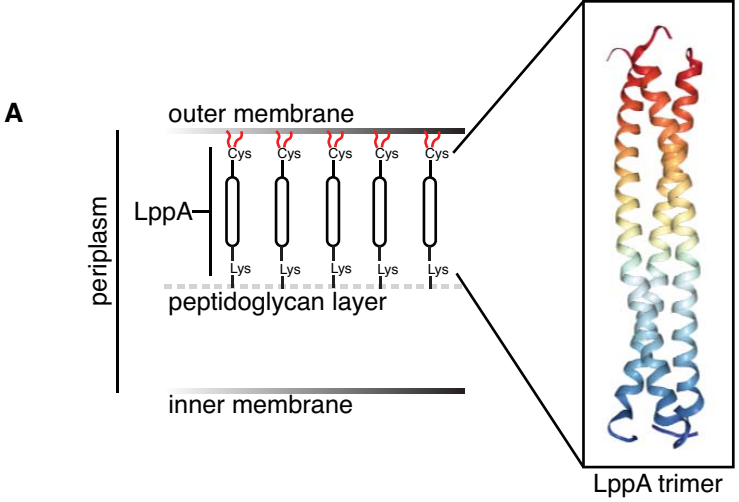

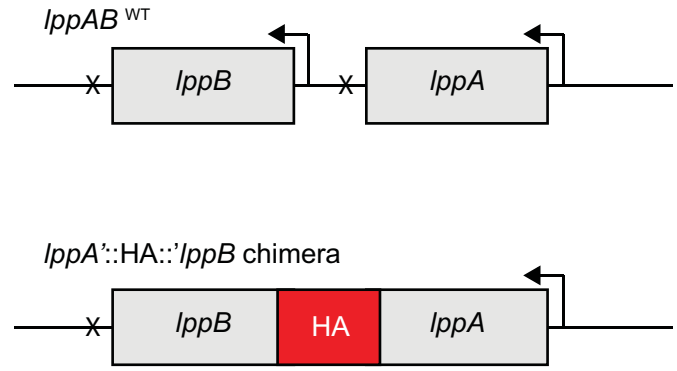

C

```
E.coli      Lpp: 1-MKATK LVLGA VILGSTLLAG CSSNAKIDQL SSDVQTLNAK
Salmonella  LppA:1-MNRTK LVLGA VILGSTLLAG CSSNAKIDQL SSDVQTLNAK
Salmonella  LppB:1-MNRTNQLILGA VVLGSTLLAG CSSNAKIDQL SSDVQTLSAK

E.coli      Lpp: 41-VDQLSNDVNA MRSDVQAAKD DAARANQRLD NMATKYRK-78
Salmonella  LppA:41-VDQLSNDVNA MRSDVQAAKD DAARANQRLD NQATKYRK-78
Salmonella  LppB:42-VEQLSNDVNA MRSDVQAAKD DAARANQRLD NKVFRICK-79
```

D

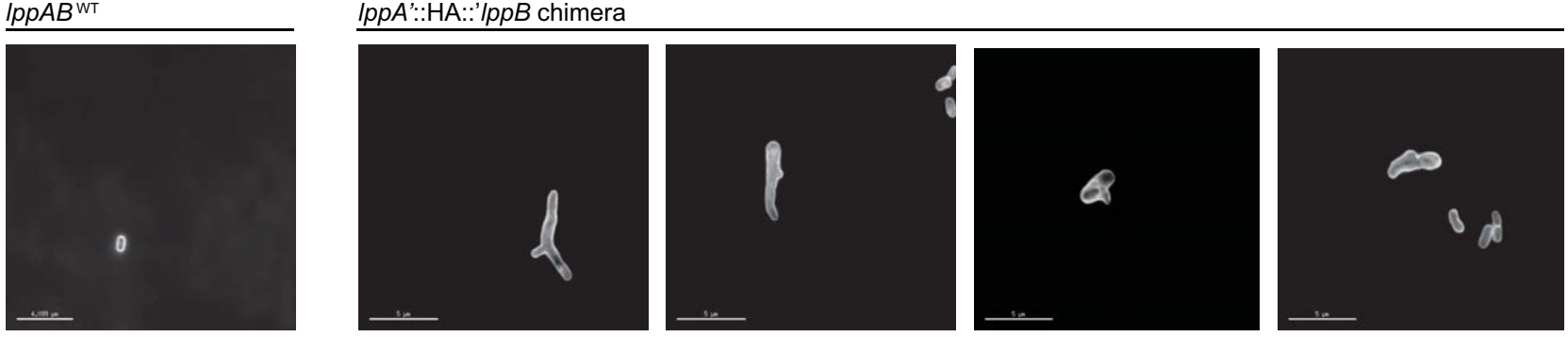

Fig. S1 Mutations in LppA can cause severe morphological defects

Mature wild type LppA is a helical tether 58 amino acids in length. The attachment of a diacylglycerol moiety to the N-terminus anchors LppA in the outer membrane, while an invariant C-terminal lysine residue is covalently bound to peptidoglycan (A). The bulk of the mature LppA protein consists of seven uninterrupted heptad repeat motifs which drive trimer formation through hydrophobic interactions between LppA molecules. We attempted to create a lengthened Lpp protein by fusing LppA to LppB with a 3x hemagluttinin (HA) tag sandwiched between the two (B). Although LppA and LppB share a high degree of homology, they have diverged considerably at their N-termini, the significance of which is unknown. Cells in this background grew very slowly and exhibited gross morphological abnormalities (D). This could have been due to the heptad repeats of the chimera being out of register, the chimera being too long or the fact that the N-termini of LppA and LppB are have diverged considerably, or all three. Ribbon structure of LppA trimer sourced from RCSB Protein Data Bank (accession #1EQ7).

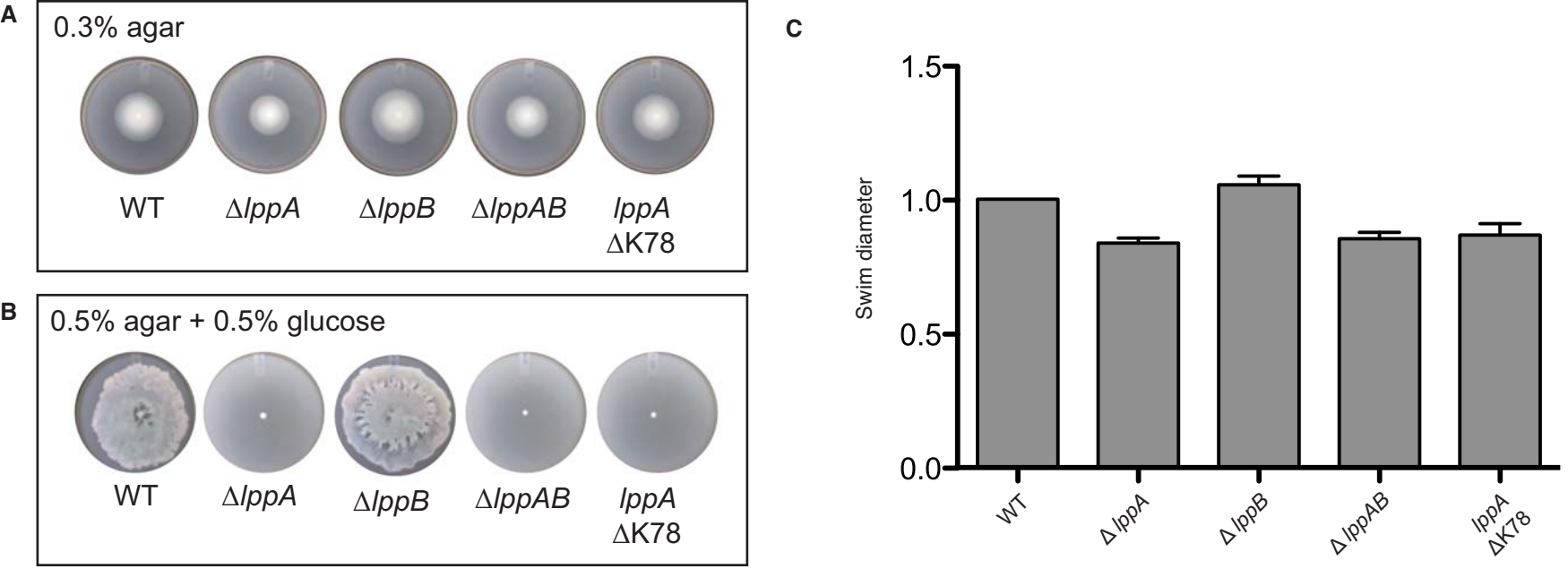

Fig. S2 Deletion of *lppA* impairs swimming motility and abolishes swarming motility

Salmonella, among other species of bacteria, exhibits two distinct forms of flagella-mediated motility: swimming and swarming. Swimming motility describes the individual behaviour of a cell swimming through liquid, while swarming is a communal behaviour whereby a swarm of flagellated bacteria moves across a hydrated surface (*35*). Swimming motility is assayed in soft agar (0.3% agar conc.), while swarming is assayed on 0.5% agar with 0.5% glucose added.

Several *lpp* deletion mutations were assayed for their effects on swimming (A) and swarming (B) motility relative to WT. Motility in swim agar was reduced ~20% in the ΔlppA, ΔlppAB and lppA ΔK78 backgrounds (C). Motility on swarm agar was abolished in the ΔlppA, ΔlppAB and lppA ΔK78 backgrounds. Deletion of lppB had little effect on either swimming or swarming motility.

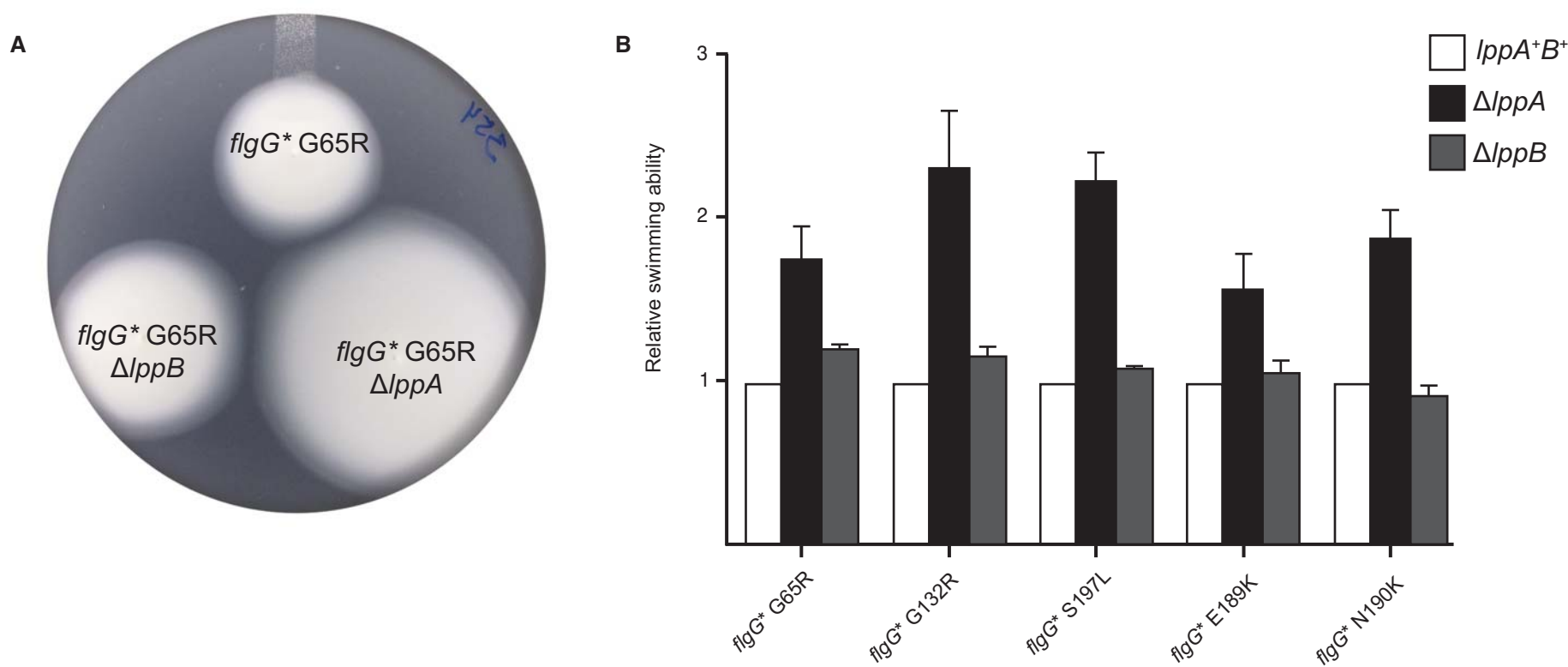

Fig. S3 Deletion of *lppA* suppressed the motility defect of *flgG mutants in soft agar**

A screen for motile *flgG** revertants produced suppressor mutations that mapped to the *lpp* operon. These suppressors were all found to affect *lppA*, the equivalent of Braun's lipoprotein in Salmonella. To verify that suppression of the *flgG** motility defect was due to loss of *lppA*, deletions of both *lppA* and *lppB* were constructed and tested for their effect on swimming motility (A). For all five *flgG** alleles tested, deletion of *lppA* resulted in a significant increase in swim diameter, while deletion of *lppB* had little to no effect (B).

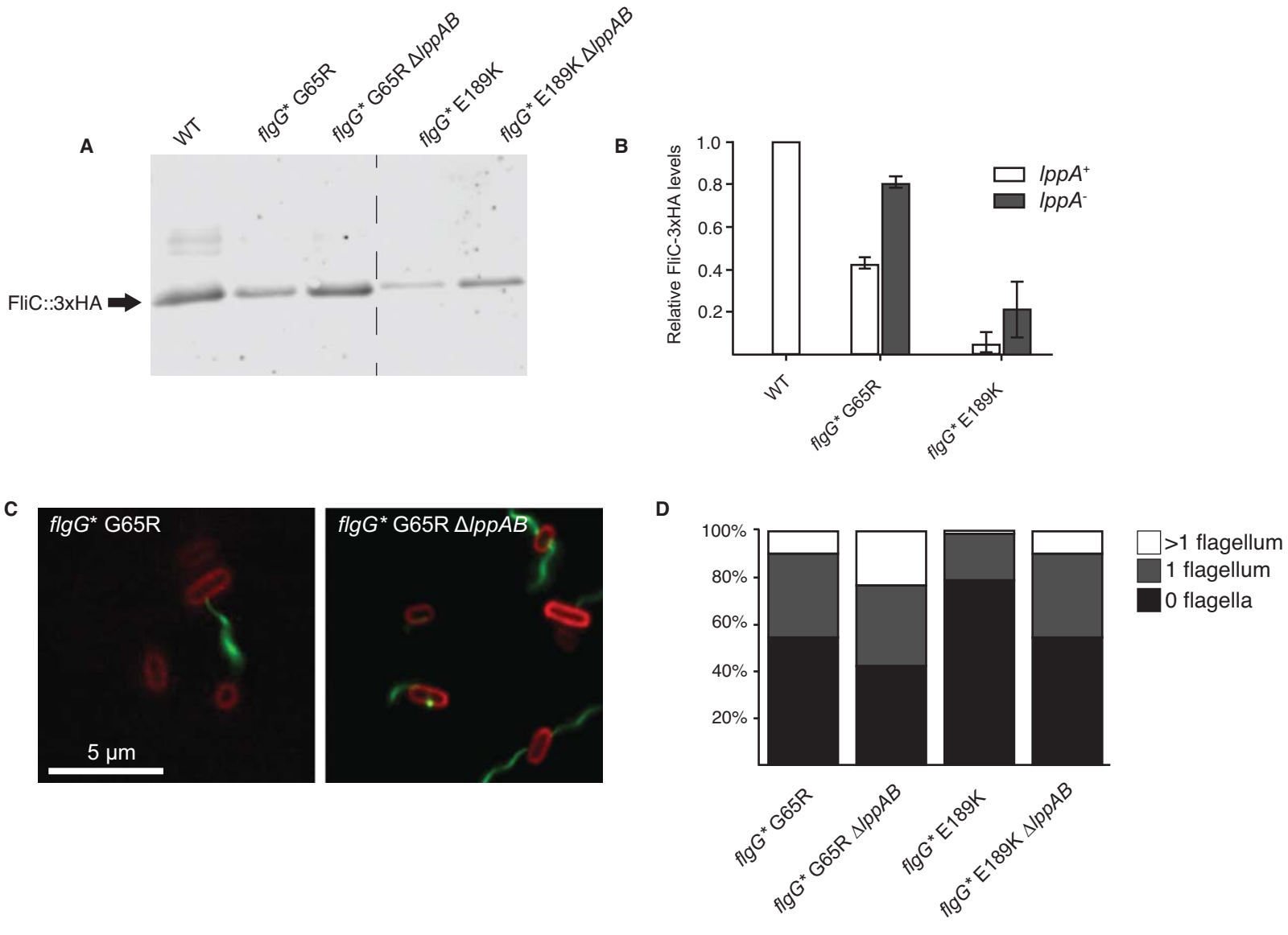

Fig. S4 Deletion of LppA increases extracellular FliC secretion and filament assembly

To determine whether deletion of LppA suppressed the motility defect of filamentous distal rod mutants by increasing the likelihood of outer membrane penetration by a *flgG** hook basal body, quantitative western blots of culture supernatants probing for 3xHA-tagged flagellin (FliC::3xHA) were performed (A and B). Loss of LppA resulted in increased FliC::3xHA secretion to the culture supernatant in the *flgG** G65R and *flgG** E189K filamentous distal rod mutant backgrounds. Fluorescence microscopy was performed using these mutants in order to count the number of extracellular formed in the presence or absence of LppA (C and D). Deletion of LppA led to greater numbers of flagellated cells, and more flagella per cell, on average, in the *flgG** G65R and *flgG** E189K filamentous distal rod mutant backgrounds.

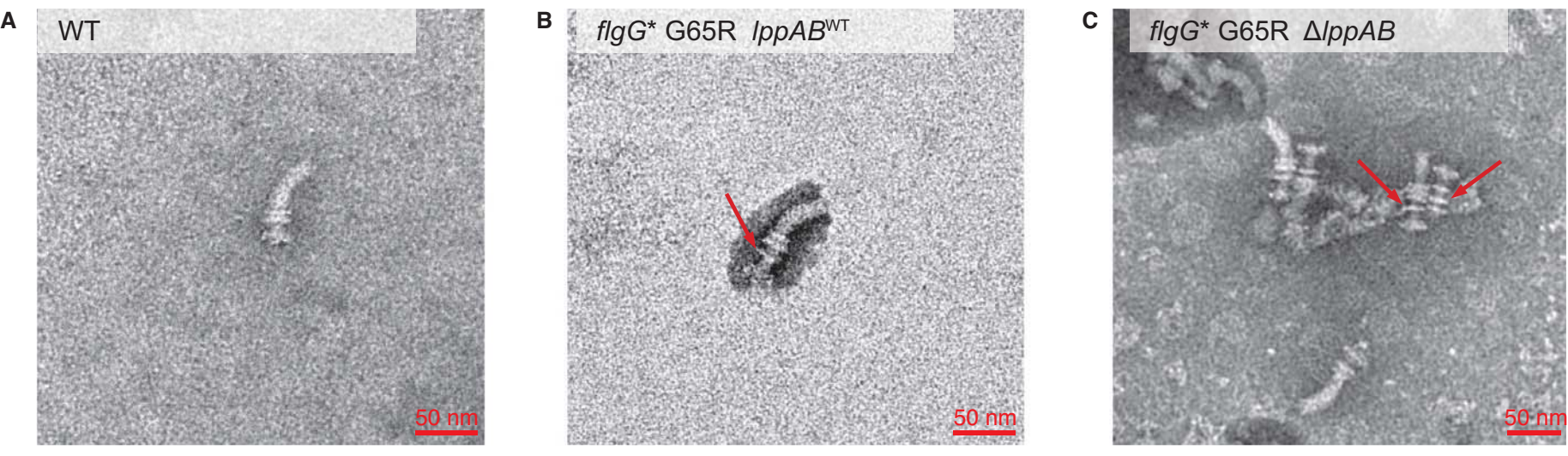

Fig. S5 Deletion of *lppAB* does not prevent filamentous rod polymerization
Hook basal bodies from WT (A), *flgG** G65R *lppAB*^{WT} (B) and *flgG** G65R Δ*lppAB* (C) backgrounds were purified, negatively stained with 2% phosphotungstic acid and examined by TEM. In both *flgG** backgrounds, cells produce filamentous rods with multiple P-rings assembled along their lengh (red arrows). This demonstrated that suppression of the *flgG** motility defect upon deletion of *lppA* was not due to prevention of filamentous rod assembly.

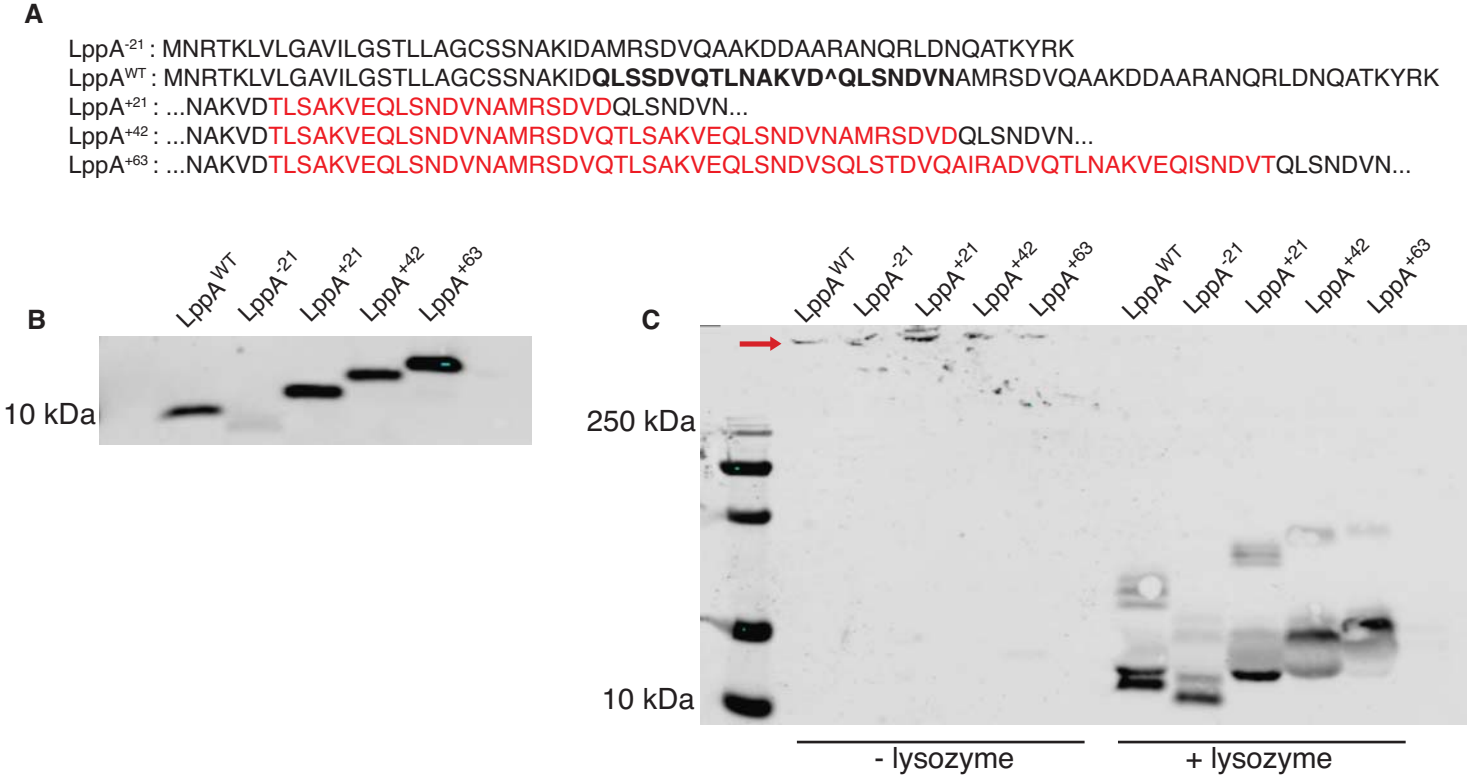

Fig. S6 Longer variants of LppA were expressed and crosslinked to the cell wall

Length variants of LppA were constructed by inserting (red lettering) or deleting heptad repeats (residues deleted from LppA^{WT} indicated with bold lettering) between residues D42 and Q43 (^) of wild type LppA (A). Western blots probing for LppA demonstrated that all length variants of LppA are expressed (B, cell lysate), secreted to the periplasm and crosslinked to the cell wall (C: purified cell sacculi with and without lysozyme digestion). In the absence of lysozyme treatment, the cell sacculus remains intact and prevents LppA crosslinked to peptidoglycan from migrating through an SDS-PAGE gel due to size exclusion (red arrow).

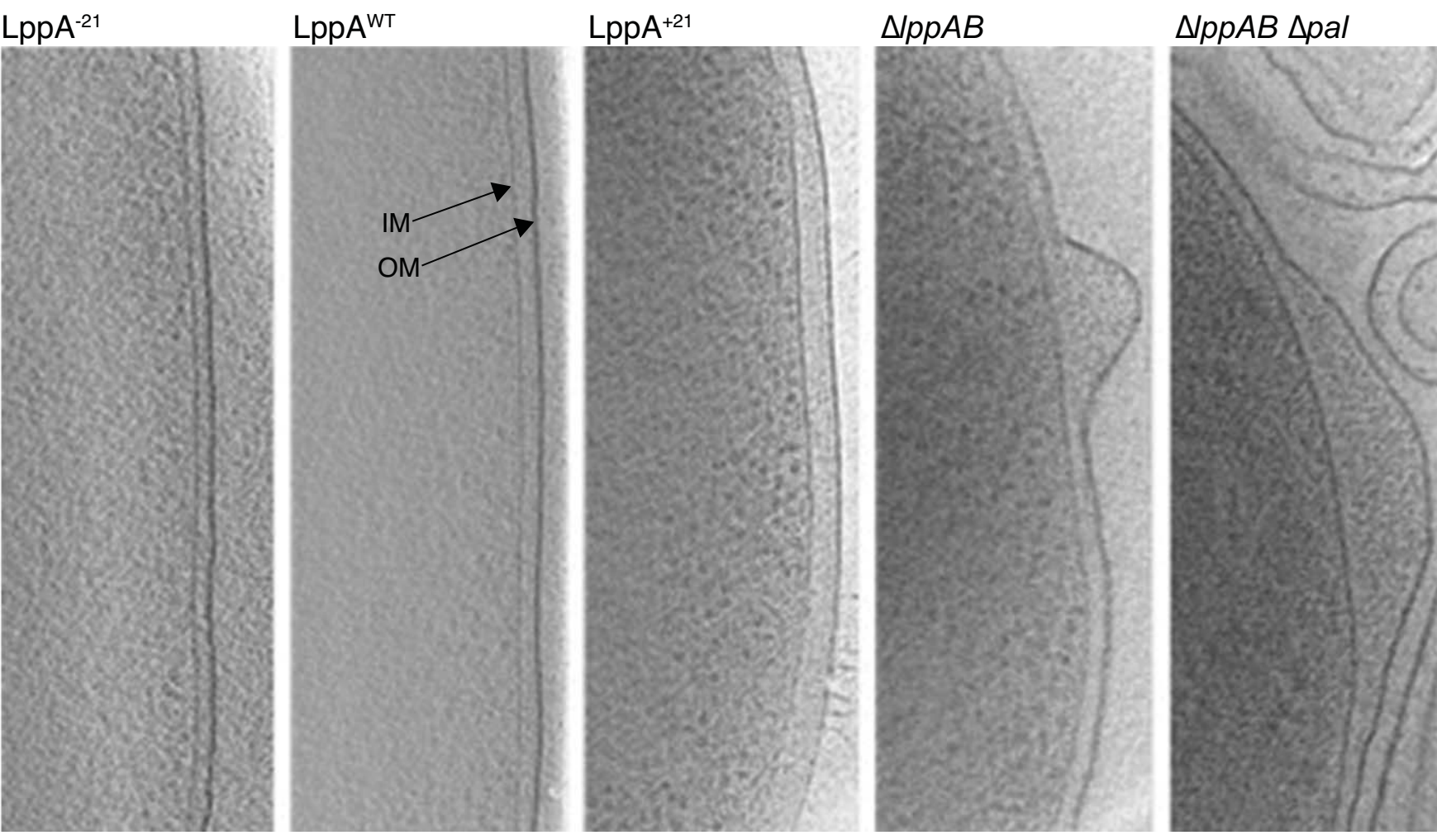

Fig. S7 LppA is a major deteminant of periplasmic spacing and outer membrane stability
Electron cryo-tomograms of frozen hydrated cells demonstrated that altering the length of LppA caused a concomitant change in inner membrane (IM) to outer membrane (OM) spacing. In the absence of LppA (Δ*lppAB*), the outer membrane pulls away, or blebs, from the cell body. The blebbing phenotype was exacerbated when *pal* was deleted in addition to *lppAB* (Δ*lppAB* Δ*pal*).

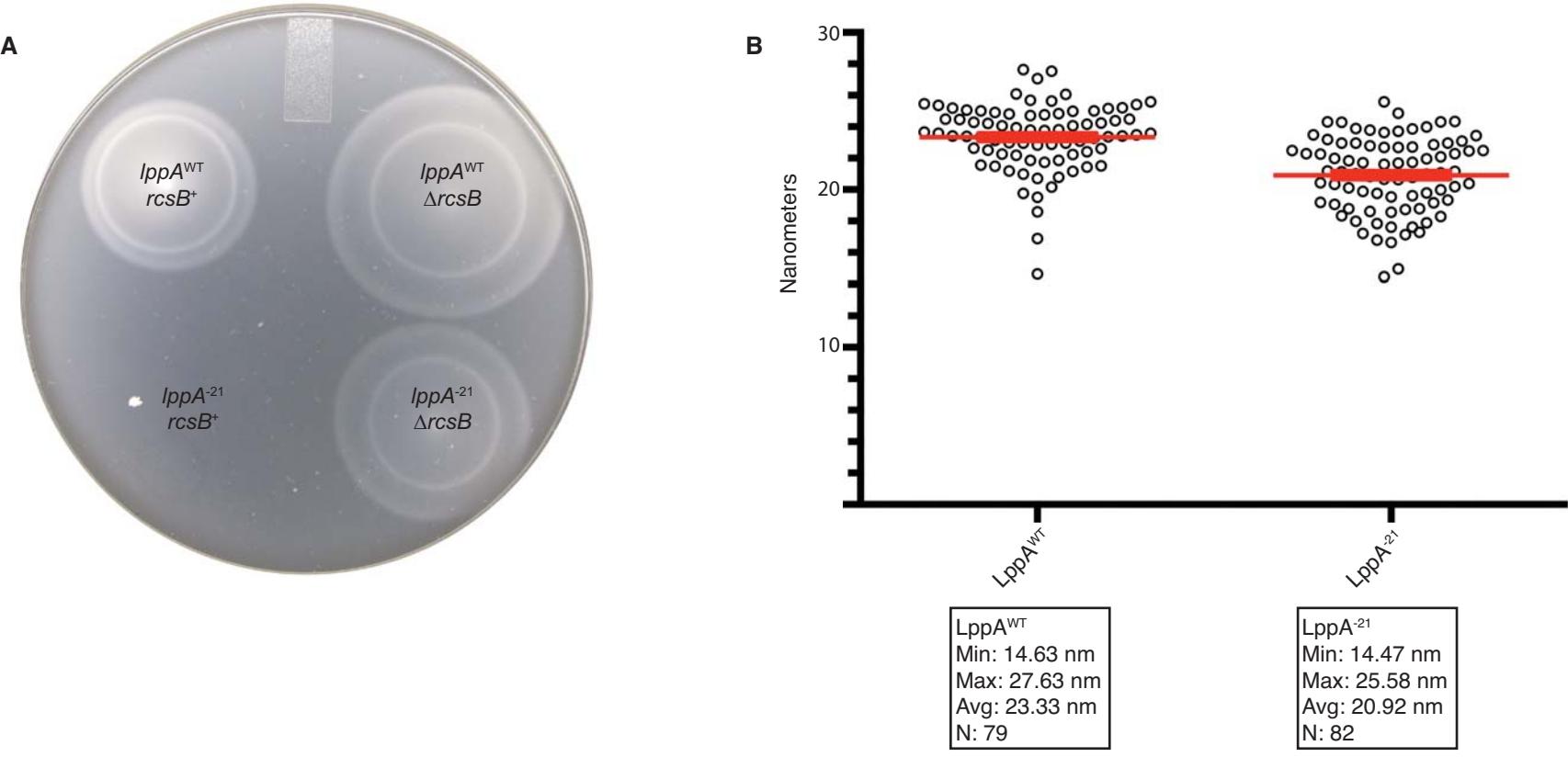

Fig. S8 Shortening LppA resulted in shorter rods

Initial attempts to isolate rods from strains harboring a length variant of LppA deleted for 3 heptad repeats ($LppA^{-21}$) were unsuccessful. Using a flagellar Class I gene transcriptional reporter (*flhC*5213::Mu*dJ*), we discovered that flagellar gene expression is repressed in $LppA^{-21}$ backgrounds (data not shown). We then knocked out known repressors of flagellar gene expression in the $LppA^{-21}$ background and assayed for motility in swim agar (0.3% agar conc.). Deletion of *rcsB*, a response regulator involved in responding to outer membrane stress, was found to restore motility to nearly wild-type levels in the $LppA^{-21}$ background (A). Rod structures were purified, negatively stained with 2% phosphotungstic acid and observed by TEM. Rods produced in the $LppA^{-21}$ were found to be shorter on average than those produced in the $LppA^{WT}$ (B, significance: $p = <0.0001$, student's two-tailed t-test, N=2, data are mean +/- SEM).

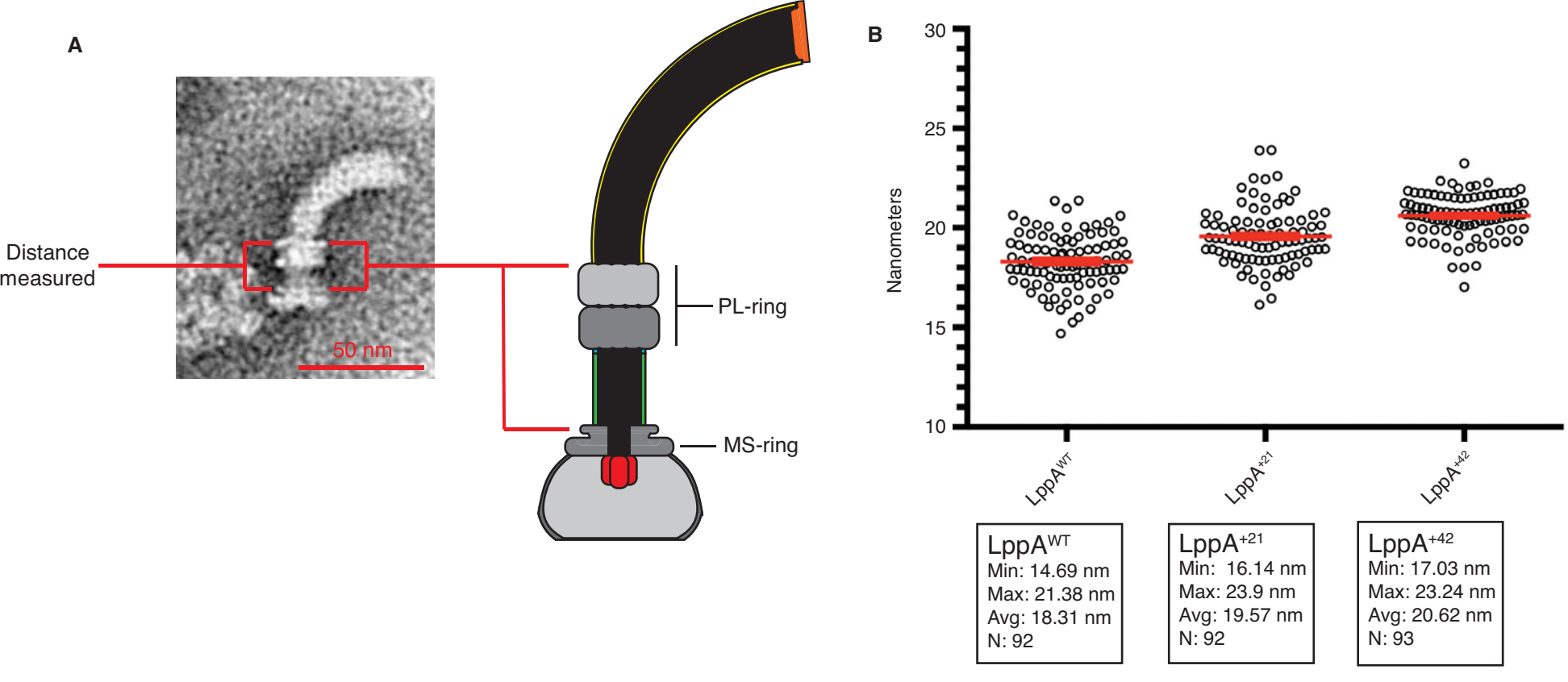

Fig. S9 Lengthening LppA increased MS-ring to PL-ring distance

Hook basal bodies (HBBs) were purified from strains expressing LppA^{WT}, LppA^{+21} and LppA^{+42} (TH22638-22640), negatively stained and observed by TEM for measurement of MS-ring to PL-ring distance (A). The distances between the top of the MS-ring to the top of the PL-ring complex (red brackets) were measured in ImageJ (NIH) and plotted using Graphpad Prism (B). The MS-ring-to-PL-ring was found to increase as the length of LppA increased (significance: p = <0.0001, one-way ANOVA, N=2, data are mean +/- SEM).

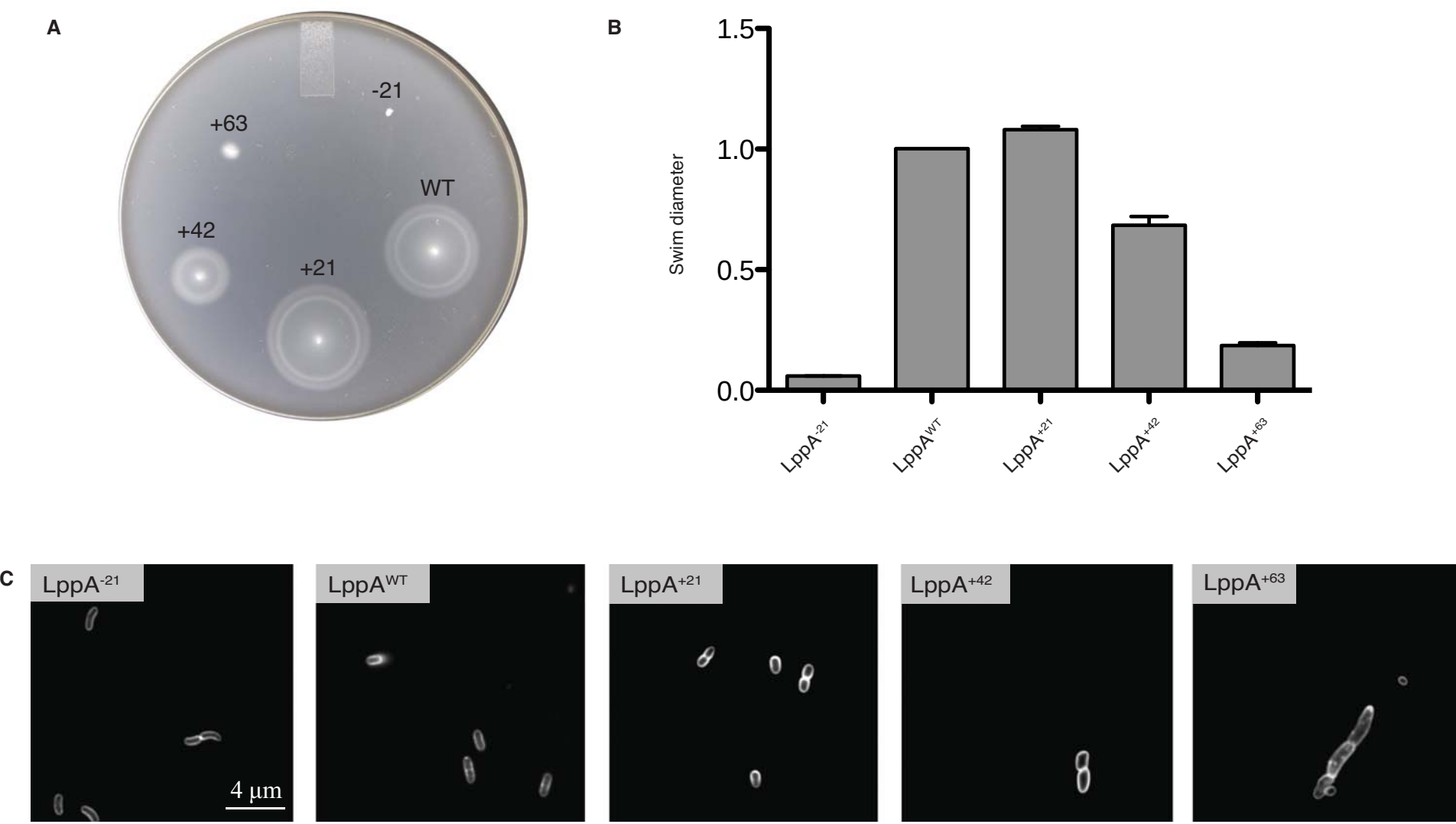

Fig. S10 Altering the length of LppA affected the swimming ability and morphology of Salmonella

The swimming ability of mutants harboring LppA length variants was assayed using soft agar swim plates (A and B). Deletion of 21 residues abolished swimming motility, while addition of 42 or 63 residues reduced the apparent swim rate relative to WT. Addition of 21 residues to LppA increased the apparent swim rate to a small degree. All length variants were unable to swarm on 0.5% swarm agar plates (not shown). Cells from each LppA length mutant were stained with FM-43 membrane dye and observed by fluorescence microscopy (C). Cell morphology became increasingly abnormal and the growth rate in liquid LB media slowed (not shown) as the length of LppA grew longer.

Table S1 List of strains used in this study

Strain	Genotype
TH437	Wild Type (LT2) strain of *Salmonella* Typhimurium
TH21911	Δ*lppAB1*::*tetRA*[a]
TH21912	Δ*lppA2*::FKF[b]
TH21913	Δ*lppB3*::FCF[c]
TH22524	Δ*flgDE7756* Δ*flgH7662* pTrc99AFF4
TH22525	Δ*flgDE7756* Δ*flgH7662* pTrc99AFF4-*flgG*$^{+}$
TH22526	Δ*lppAB1*::*tetRA flgG6705* (G65R)
TH22527	Δ*lppAB1*::*tetRA flgG6706* (G132R)
TH22528	Δ*lppAB1*::*tetRA flgG6707* (S197L)
TH22529	Δ*lppAB1*::*tetRA flgG6764* (E189K)
TH22530	Δ*lppAB1*::*tetRA flgG6750* (N190K)
TH22531	Δ*lppA2*::FKF *flgG6705*
TH22532	Δ*lppA2*::FKF *flgG6706*
TH22533	Δ*lppA2*::FKF *flgG6707*
TH22534	Δ*lppA2*::FKF *flgG6764*
TH22535	Δ*lppA2*::FKF *flgG6750*
TH22536	Δ*lppB3*::FCF *flgG6705*
TH22537	Δ*lppB3*::FCF *flgG6706*
TH22538	Δ*lppB3*::FCF *flgG6707*
TH22539	Δ*lppB3*::FCF *flgG6764*
TH22540	Δ*lppB3*::FCF *flgG6750*
TH22543	Δ*lppAB7*[d]
TH22549	Δ*lppB3*::FCF *lppA11*[e] (*lppA*$^{+21}$)
TH22550	Δ*lppB3*::FCF *lppA12*[f] (*lppA*$^{+42}$)
TH22551	Δ*lppB3*::FCF *lppA13*[g] (*lppA*$^{+63}$)
TH22552	Δ*lppB3*::FCF Δ*lppA14*[h] (*lppA*$^{-21}$)
TH22553	*fliC7746*::3xHA Δ*hin5717*::FRT *flgG6705*
TH22554	*fliC7746*::3xHA Δ*hin5717*::FRT *flgG6706*
TH21732	*fliC7746*::3xHA Δ*hin5717*::FRT *flgG6707*
TH21733	*fliC7746*::3xHA Δ*hin5717*::FRT *flgG6764*
TH21734	*fliC7746*::3xHA Δ*hin5717*::FRT *flgG6750*
TH22555	*fliC7746*::3xHA Δ*hin5717*::FRT *flgG6705* Δ*lppAB1*::*tetRA*
TH22556	*fliC7746*::3xHA Δ*hin5717*::FRT *flgG6706* Δ*lppAB1*::*tetRA*
TH22557	*fliC7746*::3xHA Δ*hin5717*::FRT *flgG6707* Δ*lppAB1*::*tetRA*
TH22558	*fliC7746*::3xHA Δ*hin5717*::FRT *flgG6764* Δ*lppAB1*::*tetRA*
TH22559	*fliC7746*::3xHA Δ*hin5717*::FRT *flgG6750* Δ*lppAB1*::*tetRA*
TH22562	Δ*lppA16* (ΔK78)[i]
TH22563	Δ*lppA16 flgG6705*
TH22564	Δ*lppA16 flgG6706*
TH22565	Δ*lppA16 flgG6707*

TH22566 Δ*lppA16 flgG6764*
TH22567 Δ*lppA16 flgG6750*
TH22568 Δ*pal*::FKF
TH22569 Δ*pal*::FKF Δ*lppAB7*
TH22574 Δ*flgDE7756* Δ*flgH7662* Δ*lppB3*::FCF Δ*prgH73*::*tetRA*
TH22575 Δ*flgDE7756* Δ*flgH7662* Δ*lppB3*::FCF Δ*prgH73*::*tetRA lppA11*
TH22576 Δ*flgDE7756* Δ*flgH7662* Δ*lppB3*::FCF Δ*prgH73*::*tetRA lppA12*
TH22577 Δ*flgDE7756* Δ*flgH7662* Δ*lppB3*::FCF Δ*prgH73*::*tetRA lppA13*
TH22578 Δ*lppAB17*::FKF[j]
TH22579 Δ*flgDE7756* Δ*flgH7662* Δ*lppB3*::FCF Δ*lppA14*
TH22580 Δ*flgDE7756* Δ*flgH7662* Δ*lppB3*::FCF Δ*rcsB139*::*tetRA*
TH22581 Δ*flgDE7756* Δ*flgH7662* Δ*lppB3*::FCF Δ*rcsB139*::*tetRA* Δ*lppA14*
TH22586 *fliC6500* (T237C) *flgG6705 motA5461*::Mu*d*J
TH22587 *fliC6500* (T237C) *flgG6764 motA5461*::Mu*d*J
TH22588 *fliC6500* (T237C) *flgG6705 motA5461*::Mu*d*J Δ*lppAB1*::*tetRA*
TH22589 *fliC6500* (T237C) *flgG6764 motA5461*::Mu*d*J Δ*lppAB1*::*tetRA*
TH22618 Δ*lppB3*::FCF Δ*rcsB139*::*tetRA*
TH22619 Δ*lppB3*::FCF Δ*rcsB139*::*tetRA* Δ*lppA14* (LppA^{-21})
TH22634 Δ*flgDE7756* Δ*flgH7662* Δ*lppB3*::FCF Δ*sseA-ssaU*::FKF Δ*prgH73*::*tetRA*
TH22635 Δ*flgDE7756* Δ*flgH7662* Δ*lppB3*::FCF Δ*sseA-ssaU*::FKF Δ*prgH73*::*tetRA lppA11*
TH22636 Δ*flgDE7756* Δ*flgH7662* Δ*lppB3*::FCF Δ*sseA-ssaU*::FKF Δ*prgH73*::*tetRA lppA12*
TH22637 Δ*flgDE7756* Δ*flgH7662* Δ*lppB3*::FCF Δ*sseA-ssaU*::FKF Δ*prgH73*::*tetRA lppA13*
TH22638 Δ*lppB3*::FCF Δ*pal*::FKF
TH22639 Δ*lppB3*::FCF Δ*pal*::FKF *lppA11*
TH22640 Δ*lppB3*::FCF Δ*pal*::FKF *lppA12*

Notes

a. *tetRA* cassette replaces *lppA* and *lppB*, leaves first 5 residues of *lppA* and last five residues of *lppB*.
b. FRT-*neo*-FRT (FKF (Km^R)) deletes all of *lppA* except for the first and last five residues.
c. FRT-*cat*-FRT (FCF (Cm^R)) deletes all of *lppA* except for the first and last five residues.
d. Clean deletion of *lppAB*, leaves first five residues of *lppA* and last five residues of *lppB*.
e. *lppA* length variant with 21 residues (3 heptad repeats) added between residues 42 and 43 of WT *lppA*.
f. *lppA* length variant with 42 residues (6 heptad repeats) added.
g. *lppA* length variant with 63 residues (9 heptad repeats) added.
h. *lppA* length variant with 21 residues (3 heptad repeats) deleted.
i. *lppA* mutant lacking the C-terminal lysine residue required for crosslinking to the cell wall peptidoglycan.
j. FKF replaces *lppA* and *lppB*, leaves first five residues of *lppA* and last five of *lppB*.

Table S2 List of primers used in this study

6572	*pal*::FXF[a] Fw	5’-attgattactaaaggaattaaagaaatgcaactgaacaaagtgtaggctggagctgcttc-3’
6573	*pal*::FXF Rv	5’-tctgaagttactgctcatgcaattctcttagtaaaccagtcatatgaatatcctccttag-3’
6574	*lppA/B*::FXF Fw	5’-taactcaatctagagggtattaataatgaatcgtactaaagtgtaggctggagctgcttc-3’
6575	*lppA/B*::FXF Rv	5’-cgccattttatattgtgcgtcaaattatttacagatgcggcatatgaatatcctccttag-3’
6576	*lpp-tetR*	5’-gttccgacgttcaggctgctaaagacgacgcagctcgcgctttaagacccactttcacat-3’
6577	*lpp-tetA*	5’-gctcagcgtctgtacatcggaagacaactgatcgattttagcctaagcacttgtctcctg-3’
6622	D*lppAB*::*tetR*	5’-ttaactcaatctagagggtattaataatgaatcgtactaaattaagacccactttcacat-3’
6623	D*lppAB*::*tetA*	5’-atgtgcgccattttatattgtgcgtcaaattatttacagatgctaagcacttgtctcctg-3’
6626	*lppB* Rv	5’-attgtgcgtcaaattatttacagat-3’
6627	*lppA* Fw 2	5’-cgctacatggagattaactcaat-3’
6645	*lppB*::FXF Fw	5’-ataaccacacaaagtataatgttattgttatgaaccgtacgtgtaggctggagctgcttc-3’
6646	*lppA*::FXF Rv	5’-cgccatttttattacgcaggtactattacttacggtatttcatatgaatatcctccttag-3’
6681	*lppA* aa42/43::*tetR*	5’-gctgtcttctgacgttcagactctgaacgctaaagttgacttaagacccactttcacat-3’
6682	*lppA* aa42/43::*tetA*	5’-gaacgtcggaacgcattgcgttcacgtcgttgctcagctgctaagcacttgtctcctg-3’
6683	*lppA*::lppB Fw	5’-ctgtcttctgacgttcagactctgaacgctaaagttgacacgctgagcgctaaagttgag-3’
6686	*lppA*::21aa-lppB Rv	5’-gaacgtcggaacgcattgcgttcacgtcgttgctcagctgatcaacgtcggaacgcattg-3’
6732	*pal* Fw	5’-ttccggcaactgatggtcag-3’
6733	*pal* Rv	5’-cgctatgccaaccagtaacga-3’
6743	*lpp1*[b] C-term tetR	5’-cacgatgtgcgccatttttattacgcaggtactattacttttaagacccactttcacatt-3’
6744	*lpp1* C-term tetA	5’-cgctaaccagcgtctggacaaccaggctactaaataccgtctaagcacttgtctcctg-3’
6788	*lpp1* -21 residues	5’-ctgcgtcgtctttagcagcctgaacgtcggaacgcat tgcatcgattttagcgttgctggagcaaccagccagcagagta-3’
7115	*lppA* Del. K78	5’-aatggcgcacgatgtgcgccatttttattacgcaggtactattaacggtatttagtagcctgg ttgtccagacgctggttagcgcgagct-3’
7188	Lpp+63 mid section	5’-ctgagcgctaaagttgagcagttgtctaacgacgttaatgcgatgcgttctgacgtccaaacattgtcagcgaaggtcgaacaattatccaac-3’
7189	Lpp+63 end section	5’-gttcaactttcgcattcagggtctgcacgtcggcacggatcgcctggacgtcggtagacagctgagagacatcgttggataattgttcgac-3’
7190	Lpp +42 mid section	5’-acgctgagcgctaaagttgagcagttgtctaacgacgttaatgcgatgcgttctgacgtccaaacattgtcagcgaaggtcgaacaattatcgaat-3’
7191	Lpp+ 63 fill	5’-gaacgtcggaacgcattgcgttcacgtcgttgctcagctgggtcacatcgttgctgatctgttcaactttcgcattc-3’
7192	Lpp+42 fill	5’-gaacgtcggaacgcattgcgttcacgtcgttgctcagctggtccacgtccgatcgcatggcatttacatcattcgataattgttcgac-3’

a: FXF is used here as an abbreviation for the FRT-Cm^R-FRT and/or FRT-Km^R-FRT antibiotic resistance cassettes

b: *lpp1* refers to *lppA*

References

1. R. M. Macnab, How bacteria assemble flagella. *Annu. Rev. Microbiol.* **57**, 77–100 (2003). doi:10.1146/annurev.micro.57.030502.090832 Medline

2. F. F. V. Chevance, K. T. Hughes, Coordinating assembly of a bacterial macromolecular machine. *Nat. Rev. Microbiol.* **6**, 455–465 (2008). doi:10.1038/nrmicro1887 Medline

3. C. J. Jones, M. Homma, R. M. Macnab, L-, P-, and M-ring proteins of the flagellar basal body of *Salmonella typhimurium*: Gene sequences and deduced protein sequences. *J. Bacteriol.* **171**, 3890–3900 (1989). doi:10.1128/jb.171.7.3890-3900.1989 Medline

4. G. J. Schoenhals, R. M. Macnab, Physiological and biochemical analyses of FlgH, a lipoprotein forming the outer membrane L ring of the flagellar basal body of *Salmonella typhimurium*. *J. Bacteriol.* **178**, 4200–4207 (1996). doi:10.1128/jb.178.14.4200-4207.1996 Medline

5. H. C. Berg, R. A. Anderson, Bacteria swim by rotating their flagellar filaments. *Nature* **245**, 380–382 (1973). doi:10.1038/245380a0 Medline

6. T. Hirano, S. Yamaguchi, K. Oosawa, S. Aizawa, Roles of FliK and FlhB in determination of flagellar hook length in *Salmonella typhimurium*. *J. Bacteriol.* **176**, 5439–5449 (1994). doi:10.1128/jb.176.17.5439-5449.1994 Medline

7. M. Erhardt, H. M. Singer, D. H. Wee, J. P. Keener, K. T. Hughes, An infrequent molecular ruler controls flagellar hook length in *Salmonella enterica*. *EMBO J.* **30**, 2948–2961 (2011). doi:10.1038/emboj.2011.185 Medline

8. K. Muramoto, S. Makishima, S. I. Aizawa, R. M. Macnab, Effect of cellular level of FliK on flagellar hook and filament assembly in *Salmonella typhimurium*. *J. Mol. Biol.* **277**, 871–882 (1998). doi:10.1006/jmbi.1998.1659 Medline

9. K. Uchida, S. Aizawa, The flagellar soluble protein FliK determines the minimal length of the hook in *Salmonella enterica* serovar Typhimurium. *J. Bacteriol.* **196**, 1753–1758 (2014). doi:10.1128/JB.00050-14 Medline

10. N. Takahashi, S. Mizuno, T. Hirano, F. F. V. Chevance, K. T. Hughes, S. Aizawa, Autonomous and FliK-dependent length control of the flagellar rod in *Salmonella enterica*. *J. Bacteriol.* **191**, 6469–6472 (2009). doi:10.1128/JB.00509-09 Medline

11. F. F. V. Chevance, N. Takahashi, J. E. Karlinsey, J. Gnerer, T. Hirano, R. Samudrala, S. Aizawa, K. T. Hughes, The mechanism of outer membrane penetration by the eubacterial flagellum and implications for spirochete evolution. *Genes Dev.* **21**, 2326–2335 (2007). doi:10.1101/gad.1571607 Medline

12. M. Homma, K. Kutsukake, M. Hasebe, T. Iino, R. M. Macnab, FlgB, FlgC, FlgF and FlgG: A family of structurally related proteins in the flagellar basal body of *Salmonella typhimurium*. *J. Mol. Biol.* **211**, 465–477 (1990). doi:10.1016/0022-2836(90)90365-S Medline

13. Y. Saijo-Hamano, N. Uchida, K. Namba, K. Oosawa, In vitro characterization of FlgB, FlgC, FlgF, FlgG, and FliE, flagellar basal body proteins of *Salmonella*. *J. Mol. Biol.* **339**, 423–435 (2004). doi:10.1016/j.jmb.2004.03.070 Medline

14. T. Fujii, T. Kato, K. D. Hiraoka, T. Miyata, T. Minamino, F. F. V. Chevance, K. T. Hughes, K. Namba, Identical folds used for distinct mechanical functions of the bacterial flagellar rod and hook. *Nat. Commun.* **8**, 14276 (2017). doi:10.1038/ncomms14276 Medline

15. T. Hirano, S. Mizuno, S. Aizawa, K. T. Hughes, Mutations in Flk, FlgG, FlhA, and FlhE that affect the flagellar type III secretion specificity switch in *Salmonella enterica*. *J. Bacteriol.* **191**, 3938–3949 (2009). doi:10.1128/JB.01811-08 Medline

16. C. J. Jones, R. M. Macnab, H. Okino, S. Aizawa, Stoichiometric analysis of the flagellar hook-(basal-body) complex of *Salmonella typhimurium*. *J. Mol. Biol.* **212**, 377–387 (1990). doi:10.1016/0022-2836(90)90132-6 Medline

17. E. J. Cohen, K. T. Hughes, Rod-to-hook transition for extracellular flagellum assembly is catalyzed by the L-ring-dependent rod scaffold removal. *J. Bacteriol.* **196**, 2387–2395 (2014). doi:10.1128/JB.01580-14 Medline

18. V. Braun, Covalent lipoprotein from the outer membrane of *Escherichia coli*. *Biochim. Biophys. Acta* **415**, 335–377 (1975). doi:10.1016/0304-4157(75)90013-1 Medline

19. A. Kovacs-Simon, R. W. Titball, S. L. Michell, Lipoproteins of bacterial pathogens. *Infect. Immun.* **79**, 548–561 (2011). doi:10.1128/IAI.00682-10 Medline

20. W. Shu, J. Liu, H. Ji, M. Lu, Core structure of the outer membrane lipoprotein from *Escherichia coli* at 1.9 Å resolution. *J. Mol. Biol.* **299**, 1101–1112 (2000). doi:10.1006/jmbi.2000.3776 Medline

21. J. Sha, A. A. Fadl, G. R. Klimpel, D. W. Niesel, V. L. Popov, A. K. Chopra, The two murein lipoproteins of *Salmonella enterica* serovar Typhimurium contribute to the virulence of the organism. *Infect. Immun.* **72**, 3987–4003 (2004). doi:10.1128/IAI.72.7.3987-4003.2004 Medline

22. A. A. Fadl, J. Sha, G. R. Klimpel, J. P. Olano, D. W. Niesel, A. K. Chopra, Murein lipoprotein is a critical outer membrane component involved in *Salmonella enterica* serovar Typhimurium systemic infection. *Infect. Immun.* **73**, 1081–1096 (2005). doi:10.1128/IAI.73.2.1081-1096.2005 Medline

23. C. Kröger, A. Colgan, S. Srikumar, K. Händler, S. K. Sivasankaran, D. L. Hammarlöf, R. Canals, J. E. Grissom, T. Conway, K. Hokamp, J. C. D. Hinton, An infection-relevant transcriptomic compendium for *Salmonella enterica* serovar Typhimurium. *Cell Host Microbe* **14**, 683–695 (2013). doi:10.1016/j.chom.2013.11.010 Medline

24. D. S. Cayley, H. J. Guttman, M. T. Record Jr., Biophysical characterization of changes in amounts and activity of *Escherichia coli* cell and compartment water and turgor pressure in response to osmotic stress. *Biophys. J.* **78**, 1748–1764 (2000). doi:10.1016/S0006-3495(00)76726-9 Medline

25. K. A. Sochacki, I. A. Shkel, M. T. Record, J. C. Weisshaar, Protein diffusion in the periplasm of E. coli under osmotic stress. *Biophys. J.* **100**, 22–31 (2011). doi:10.1016/j.bpj.2010.11.044 Medline

26. E. Cascales, A. Bernadac, M. Gavioli, J.-C. Lazzaroni, R. Lloubes, Pal lipoprotein of *Escherichia coli* plays a major role in outer membrane integrity. *J. Bacteriol.* **184**, 754–759 (2002). doi:10.1128/JB.184.3.754-759.2002 Medline

27. L. M. Parsons, F. Lin, J. Orban, Peptidoglycan recognition by Pal, an outer membrane lipoprotein. *Biochemistry* **45**, 2122–2128 (2006). doi:10.1021/bi052227i Medline

28. T. Nambu, T. Minamino, R. M. Macnab, K. Kutsukake, Peptidoglycan-hydrolyzing activity of the FlgJ protein, essential for flagellar rod formation in *Salmonella typhimurium*. *J. Bacteriol.* **181**, 1555–1561 (1999). Medline

29. K. A. Datsenko, B. L. Wanner, One-step inactivation of chromosomal genes in *Escherichia coli* K-12 using PCR products. *Proc. Natl. Acad. Sci. U.S.A.* **97**, 6640–6645 (2000). doi:10.1073/pnas.120163297 Medline

30. S. I. Aizawa, G. E. Dean, C. J. Jones, R. M. Macnab, S. Yamaguchi, Purification and characterization of the flagellar hook-basal body complex of *Salmonella typhimurium*. *J. Bacteriol.* **161**, 836–849 (1985). Medline

31. D. N. Mastronarde, Correction for non-perpendicularity of beam and tilt axis in tomographic reconstructions with the IMOD package. *J. Microsc.* **230**, 212–217 (2008). doi:10.1111/j.1365-2818.2008.01977.x Medline

32. D. N. Mastronarde, Automated electron microscope tomography using robust prediction of specimen movements. *J. Struct. Biol.* **152**, 36–51 (2005). doi:10.1016/j.jsb.2005.07.007 Medline

33. C. Suloway, J. Shi, A. Cheng, J. Pulokas, B. Carragher, C. S. Potter, S. Q. Zheng, D. A. Agard, G. J. Jensen, Fully automated, sequential tilt-series acquisition with *Leginon*. *J. Struct. Biol.* **167**, 11–18 (2009). doi:10.1016/j.jsb.2009.03.019 Medline

34. J. R. Kremer, D. N. Mastronarde, J. R. McIntosh, Computer visualization of three-dimensional image data using IMOD. *J. Struct. Biol.* **116**, 71–76 (1996). doi:10.1006/jsbi.1996.0013 Medline

35. D. B. Kearns, A field guide to bacterial swarming motility. *Nat. Rev. Microbiol.* **8**, 634–644 (2010). doi:10.1038/nrmicro2405 Medline